

## N O T I C E

THIS DOCUMENT HAS BEEN REPRODUCED FROM  
MICROFICHE. ALTHOUGH IT IS RECOGNIZED THAT  
CERTAIN PORTIONS ARE ILLEGIBLE, IT IS BEING RELEASED  
IN THE INTEREST OF MAKING AVAILABLE AS MUCH  
INFORMATION AS POSSIBLE

ACOUSTIC EMISSION MONITORING  
OF POLYMER COMPOSITE MATERIALS  
II. EXPERIMENTAL RESULTS

R. Bardenheier

(NASA-TM-76523) ACOUSTIC EMISSION  
MONITORING OF POLYMER COMPOSITE MATERIALS  
(National Aeronautics and Space  
Administration) 29 p HC A03/MP A01 CSCL 11D

N81-20187

Unclas

G3/24 41864

Translation of "Schallemissionsuntersuchungen an polymeren Verbundwerkstoffen.  
Teil II. Experimentelle Ergebnisse," Zeitschrift fuer Werkstofftechnik, Vol. 11,  
March 1980, pp 101-110



NATIONAL AERONAUTICS AND SPACE ADMINISTRATION  
WASHINGTON, D.C. FEBRUARY 1981

1. Report No. NASA TM-76523	2. Government Accession No.	3. Recipient's Catalog No.	
4. Title and Subtitle ACOUSTIC EMISSION MONITORING OF POLYMER COMPOSITE MATERIALS		5. Report Date February 1981	6. Performing Organization Code
		8. Performing Organization Report No.	
7. Author(s) Reinhard Bardenheier		10. Work Unit No.	
		11. Contract or Grant No. NASw- 3199	
9. Performing Organization Name and Address Leo Kanner Associates, Redwood City, California 94063		13. Type of Report and Period Covered Translation	
		14. Sponsoring Agency Code	
12. Sponsoring Agency Name and Address National Aeronautics and Space Adminis- traion, Washington, D.C. 20546			
15. Supplementary Notes Translation of "Schallemissionsuntersuchungen an polymeren Verbundwerkstoffen, Teil II. Experimentelle Ergebnisse," Zeitschrift fuer Werkstofftechnik, Vol. 11, March 1980, pp 101-110  (A80-30581)			
16. Abstract The technique of acoustic emission monitoring of polymer com- posite materials is described. It is a highly sensitive, quasi-nondestructive testing method that indicates the origin and behavior of flaws in such materials when submitted to different load exposures. With the use of sophisticated signal analysis methods it is possible to distinguish between different types of failure mechanisms, such as fiber fracture, delamination or fiber pull-out. Imperfections can be detect- ed while monitoring complex composite structures by acoustic emission measurements.			
17. Key Words (Selected by Author(s))		18. Distribution Statement  Unlimited - Unclassified	
19. Security Classif. (of this report)  Unclassified	20. Security Classif. (of this page)  Unclassified	21. No. of Pages	22.

ACOUSTIC EMISSION MONITORING  
OF POLYMER COMPOSITE MATERIALS

II. Experimental Results  
R. Bardenheier

Composite Materials -- Characteristics and Failure Mechanisms

The designation "composite materials" denotes a class of materials in which two or more components are mutually "compounded" in a suitable manner in order to generally improve product properties. Thus, e.g., fig. 10 clearly shows the reinforcing and strengthening effects of short glass fibers imbedded in a styrene-acrylnitril copolymer matrix (SAN) [24]. It shows the mechanixal behavior of this composite material during monotonous increase of stress effects ( $\dot{\epsilon} \approx 10^{-3} \text{s}^{-1}$ ) in relation to glass fiber contents. While strength and the initial tangential modulus increase in comparison to the corresponding properties of the unreinforced matrix (0%GF), the deformability as well as the specific deformation energy of the composite materials decrease. However, in no case can it be deduced from the stress-strain curves whether at a specific point of time the first defects have already occurred and what will their behavior be under continued exposure to stress effects. All curves show a degressive progress without indicating points of instability in damage to the materials. On the other hand, simultaneously conducted SE-measurements have shown energy transformation processes occurring early in the samples, thus pointing up irreversible damage to materials (fig. 11). This illustration shows that SE-measurements can provide overall information regarding the stress state of and the degree of damage to a composite material. Nevertheless, to achieve

---

\*Numbers in the margin indicate pagination in the foreign text.

optimization of materials, it is additionally necessary to differentiate between the various failure mechanisms so as to apply appropriate measures against all weak points.

As shown in fig. 12, failure mechanisms in composite materials are very complex, as fibre fracture 1, matrix fracture and matrix crazing 2, as well as fiber pull-out without 3 and with matrix yielding 4 can occur simultaneously. Each of these mechanisms contributes its share to overall emission, whereby consideration /102 must also be given to friction margin frictions. This makes differentiation between these various failure mechanisms as well as the corresponding coordination of SE-signals difficult and costly. Yet, as will be shown, it is not an impossible task.

Swindlehurst and Engel 25 developed a theoretical system for describing SE in composite materials. They start out with the assumption that the failure of a brittle component, generally the reinforcing fibers, leads to a recordable emission of elastic stress waves. At the same time they give in their model due consideration to interaction among the components. They show that this relaxation of the fractured fibers is connected to an additional stress, i.e., deformation of the matrix. According to their theoretical postulations, occurrence of SE is characterized, among others, also by the degree of matrix deformation.

Propagation of sound waves conducted in composite materials, as well as the elastic stress waves (SE), are described by Barker 26 . In his deliberations he takes into consideration a visco-elastic behavior of the composite entity corresponding to that of a Maxwell body. Resonance effects are excluded by him.

## Acoustic Emission Measurements on Composite Materials with a Polymer Matrix

### Monotonous Stress Increase

#### Interpretation of Acoustic Emission Signals

A quantitative relationship between fiber fracture as a failure phenomenon and the recorded SE is shown by Harris et al [27] for an aluminum matrix reinforced by adjusted  $Al_3Ni$ -whiskers (fig. 13). (Though they studied a metallic composite material, their study contains an interesting concept for quantitative description of the SE-characteristic of this material.) They started out with the assumption that only fiber fractures contribute to the recorded SE, while the matrix is to be considered as "quiet." In their theoretical model they assume that the amount of energy released in case of a fiber fracture is proportionate to the square of the fiber load tension at the point of time when the fracture occurs. The equation derived by them makes it possible to establish a quantitative correlation between the percentual, experimentally determined number of fiber fractures ( $\omega$ ) and the sum of pulses (N) of SE (fig. 13):

$$N = B \cdot \int_{\epsilon_0}^{\epsilon} \frac{d}{d} \cdot \ln \frac{\epsilon}{\epsilon_0} \cdot d\epsilon;$$

B is a proportionality constant and  $\epsilon_0$  the stress at which the first emissions are recorded.

A similar finding was reached also by Rotem and Baruch [28], who studied an epoxy resin matrix (UD-GF/EP) reinforced by unidirectional oriented glass fibers. While they do not derive any

analytic relation between fiber fractures and the sum of SE pulses, they computed the relative incidence of fractured fibers ( $F(\sigma_f)$ ) and pointed out a qualitative relationship with the sum of SE pulses ( $N$ ) (fig. 14). They formulated the function  $F(\sigma_f)$  under the assumption of a statistic distribution of glass fiber strength. The viscoelastic behavior of the epoxy resin matrix is included in the discussion of their studies. They make it responsible for the steep rise of the pulse sum curve of SE ( $N$ ) in the terminal stage, i.e., at a high stress level. Due to relaxation processes in the matrix, are included to an ever increasing degree in transfer of force which simultaneously increases the probability of fiber fracture. They do not specify any relationship between SE and some material characteristic.

Liptai [29] also reports on a relationship between SE pulse sum measurements and fracture of high-strength glass fibers. He studied NOL-rings (Naval Ordnance Laboratory) made of glass fiber/epoxy resin composites. For the description of fiber fracture he used the concept theoretically derived by Zweben and Rosen [30] which predicts a cumulative fiber failure in relation to fiber exposure to stress.

A correlation between fiber fracture and critical surface- or fracture-energy ( $\gamma_c$ ) is reported by Fitz-Randolph et al. [31, 32], who conducted studies on notched epoxy resin samples reinforced by boron fibers. Due to the selection of a suitable sample configuration they succeeded in producing a steady crack propagation under monotonously increasing stress effects.  $\gamma_c$  was determined by means of the "compliance method" described in [33]. At stress applied

perpendicularly to the fiber orientation (fig. 15) they observed with each load drop, accompanied by crack propagation, a distinct SE-burst. By means of simultaneously performed electric resistance measurements they showed that these bursts were caused by fiber fractures. As fig. 15 shows, there is a direct relationship between the sum of SE pulses ( $N^*$ ) and the critical surface energy ( $\gamma_c$ ) when both of these values are related to the given crack surface. The dependence of value  $\gamma_c$ , and thus of  $N^*$ , on the crack surface ( $A$ ) is ascribed by the authors to the varying fiber pull-out length which decreases with increasing crack length.

While they do not offer an explanation for the variation in fiber pull-out length, newer studies by Harris and Ankara [34] show that friction processes occur during fiber pull-out between the glass fibers and the matrix, which largely contribute to the total fracture energy. This can be used to explain the dependence of critical surface energy on the fiber pull-out length observed by Fitz-Randolph et al. [31, 32]. Harris and Ankara carried out their studies on a polyester cantilever beam (DCB-probe) and were in a position to differentiate between processes in the matrix and those in the glass fibers or the boundary surface.

Fiber fractures, however, are not the only failure phenomena in composite materials. This is graphically represented in fig, 12. Mehan and Mullin [35] describe experiments with carbon fiber/ and boron /104 fiber/epoxy resin composites which allowed them to use SE-signal analyses to differentiate between fiber breakdown, matrix breakdown and boundary surface failure. They also point out the difficulties connected with the interpretation of the individual signal forms, as sample size as well as composite makeup affect the frequency contents of the emitted signals.

Wolitz et al. [36] show that the signals emitted during fiber fractures are more intensive by approximately 15 dB than those due to intermediate fiber fractures.<sup>1</sup> Fig. 16 and 17 shows pictures taken by a scanning electron microscope of both failure types coordinated with the time signals of the corresponding SE. In compliance with the theory of Fourier's transformation, it can be deduced from the frequency spectrum of the signals that short signal pulses generated by fiber fractures show a high frequency spectrum (fig. 16). Delamination processes (intermediate fiber breakdowns) in the form of long lasting signals show, on the other hand, a spectrum quickly dying-out to high frequencies (fig. 17).

These findings are analogous to the amplitude analysis [20] reported on in [36-40]. Depending on the amplitude height of signals measured by means of a variable discriminator, the cumulative amplitude distribution for discontinuous emissions can be computed, according to Jax [41], according to the equation

$$I = I_0 \cdot D^{-n}$$

wherein I denotes the cumulative amplitude frequency, D the discriminator, and  $I_0$  and n positive constants; in cumulative amplitude distribution, all processes taking place above the selected discrimination limit are counted. Under these conditions, the exponent n for failure processes due to delamination and fiber fracture takes on different values which are outlined for various composite systems in table 1. As, however, these two failure mechanisms do not occur separately, but overlap, the exponent can be determined only relatively.

---

1 As it is difficult in the case of complex composite materials to differentiate failure mechanisms occurring outside of reinforcement fibers (fig. 12; process 2, 3 and 4), these are combined under the term "delamination."

The amplitude distribution curves are valuable as sources of information regarding the energy density of SE signals. As a representation of the time signal of a fiber fracture shows in fig. 16, the convertor in this type of failure is excited to oscillations with a higher number of high signal amplitudes. Contrarily, the time signal of delamination shows only low signal amplitudes (fig. 17). Both failure mechanisms differ therefore in a characteristic way in their signal amplitudes. As an example, fig. 18 shows the cumulative amplitude distribution of SE signals [20, 36] analyzed during a burst-pressure test on a GFK-container. Table 1 shows that the exponent  $n$ , and, thus, the slope of the line in fig. 18, decreases in direct proportion to the energy richness of the SE signal. The change in the line slope lying between pressure points 450 and 480 indicates the described change of primary damage processes from delamination to fiber fracture.

To facilitate differentiation between the two in experimental studies of various failure mechanisms, use is generally made of unidirectionally reinforced samples which are exposed to stress perpendicularly as well as parallel to fiber-, i.e., reinforcement-direction. The effects of the matrix- and reinforcement-material as well as the fiber orientation on the SE-characteristic of polymer composites are dealt with by Roeder and Crostack [42]. Their mechanical and SE-studies of epoxy- (EP) and polyester resin matrixes (UP) reinforced with carbon fibers (CF) and glass fibers (GF) show that boundary adhesion between the two composite components plays an important role. As examples serve the findings for CF/EP- and CF/UP-composites with fiber orientation perpendicular to the direction of stress (fig. 19a, b). While the adhesion

between the two components in the CF/UP composite undergoes quasi intermittent damaging, in the case of CF/EP composites sets in early a relatively continuous damage process detectable by SE measurements. The latter in its early stages can be primarily ascribed to formation of microfractures in the matrix. The SE curve of the CF/EP composite shows in comparison to the CF/UP composite a "more ductile" material behavior. SE measurements provide information about the damaging process even in the case of composites exposed to stress in parallel to the direction of reinforcement. Fig. 19 shows the stress ( $\sigma$ ) and the sum of pulses of SE (N) for a CF/UP composite. The steep rise of the pulse sum curve denotes failure of the carbon fibers.

Liptai [29] also came to a similar conclusion in regards to the effects of fiber orientation on the SE characteristic of epoxy resin samples reinforced with glass fibers unidirectionally. He conducted pressure tests on cylindrical samples and, in the case of samples with glass fibers in parallel to the direction of stress, recorded only a single fracture which occurred only in the matrix without crossing a single glass fiber. Shortly prior to the failure there set in a limited SE activity (fig. 20). On the other hand, a progressive SE characteristic in a fiber orientation transversal to the direction of stress gave an early indication of damage processes which eventually resulted in a breakdown progressing at a plane  $45^\circ$  below the axis of stress (fig. 20).

However, in practice one encounters often multiaxial stress fields that cannot be taken up by a single unidirectionally reinforced layer. Constructively this is counteracted by multilayer

composites consisting of several layers with differing orientation of fibers. Among others, Roeder et al. [37, 38] show that it is also possible to specify the total breakdown of these composites in regards to differing damage mechanisms -- as delamination and/or fiber fracture -- by the described analytical process. As shown in fig. 21, the metrologically simple representation of the sum of SE pulses (N) is well suited for monitoring the total damaging progress in multilayer composites. The studies involved a number of composites with differing reinforcement arrangements with an externally located mat layer as well as a mat laminate. The ratio of reinforcement from transverse direction to that of stress was  $V = 1:1.2$  and  $1:2$ . /106

Weyhreter and Korak [43] propose a concept that makes it possible to estimate the ultimate strength from the sum of SE pulses at a given stress. They verified and confirmed this concept on glass fiber/epoxy resin samples and carbon fiber/epoxy resin components. In their reasoning they started out with a statistical distribution of strengths of composite materials expressed by the SE characteristic; a way of reasoning that has already been the subject of discussions [28, 30].

#### Effects of Defects on SE Characteristic

The effects of depressions, defective and weak spots on mechanical behavior and SE characteristic of composite materials has been described in various studies.

Fuwa et al. [44] studied indented and not-indented epoxy resin samples in tensile tests and found a higher SE activity in indented

samples than in not indented samples. They ascribed this to the stress peaks in indentation that caused a premature tangential stress failure parallel to the fibers.

Speake and Curtis [45] observed in epoxy resins reinforced by carbon fibers a displacement of the frequency spectrum of the emitted signals of 0-70 kHz in the case of non-indented samples and in the 30-130 kHz range in the case of indented samples. In conformance with this finding, Williams and Lee [46], using a carbon fiber/epoxy resin composite provided with artificial defects in its multiple layers, show that samples with defects reveal proportionately more failure mechanisms with greater energy release rates than nondefective samples. According to the data contained in fig. 17, 17 and 18, following the laws of Fourier's transformation [36], signal displacement into higher-frequency spectral ranges indicates occurrence of processes in a constantly decreasing span emitting SE with increasing amplitudes. Consequently, fiber fractures are to be regarded as the most probable failure mechanisms.

Becht et al [39] report on bursting stress tests with wound glass fiber/epoxy resin tubes with interior lining. They observed that defective pipes showed a distinctly higher SE activity than tubes without defects (fig. 22). In the case of these composites consisting of nine individual layers, artificial defects were introduced into the three middle layers, such as fiber fractures or roving knots. Fig. 22 shows that defective tubes register SE very early (from approximately 50 bar) which constantly increase in their incidence from approximately 500 bar. On the other hand, in the case of defect-free tubes, SE activity does not set in until internal

pressure has reached approximately 200 bar and remains at a low level throughout the duration of the experiment.

Hamstad and Chiao [47] report that while SE measurements are suitable for indicating defects in containers with multiple-layer winding, they presuppose that the defect decisively affects the container strength. According to their investigations, such defects could be proven by SE measurements in approximately 50% of failure tests, while noncritical defects could hardly be detected through SE.

The problem of possible pinpointing of defects in composite materials is dealt with by Schwalbe [48]. He shows that localized defects can be detected by means of linear location methods, even though sound wave propagation in these materials is anisotropic. He specifies pinpointing accuracy at 5%. He estimates the type of defect by means of simultaneously performed pulse sum measurements of SE.

#### Damage Assessment with a View to Time Effects

/107

Effects of creep rate on SF behavior of composite materials were studied by Rotem [49] in a range of two decimal powers. He shows that unidirectionally reinforced carbon fiber/epoxy resin composites give no indication of dependence of SE activity on the creep rate, while the opposite is true of unidirectionally reinforced glass fiber/epoxy resin composites. As an explanation Rotem offers the differences in the elasticity modulus of both reinforcement materials. On the basis of varying E-moduli (table 2), same external stress produces a stronger stress elevation in proximity of glass fibers rather than carbon fibers. The matrix responds to

this additional stress by formation of microcracks, leading to additional SE [25]. In the case of glass fiber/epoxy resin composites Rotem observed increase in SE activity with decreasing creep rate.

Studies by Rotem and Baruch [28] as well as Hahn and Kim [50] show that SE measurements can also be successfully used in time lapse experiments for monitoring the damage progress in unidirectionally reinforced GFK-samples exposed to constant stress. Monotonously increasing stress application produces a progressively increasing SE activity shown in fig. 23 in the form of pulse rate representation of SE (N) over the stress exposure time (t). As pointed out in [28], these SE are due to fiber fractures. As soon as the load is kept constant, the pulse rate does immediately abate, but never disappears completely. As possible explanation for this phenomenon Rotem and Baruch [28] offer the viscoelastic properties of the matrix. Due to high exposure to stress ( $\sigma = 758 \text{ N/mm}^2 = 0.85 \cdot \sigma_B$ ), the epoxy resin matrix is exposed to a high stress concentration in its fiber range, which it tries to counter by formation of microcracks as well as by stress relaxation. This produces additional stress on glass fibers so that isolated fiber fractures occur even though the load is kept constant. The impending material failure manifests itself then immediately prior to breakdown by intensive SE activity.

The time span tests conducted by Goettlicher [51] on SAN-copolymers reinforced with short glass fibers coincide with the above observations. At a stress level of  $0.9 \cdot \sigma_B$  the median test duration is 11 hours. Over a time span of approximately 2 hours an increasingly intensive SE activity indicates sample failure.

Effects of ageing processes on the mechanical properties of glass fiber/polyester resin and glass fiber/epoxy resin composites were studied by Crostack and Roeder [52]. SE measurements made simultaneously on aged and non-aged samples showed this method to be very sensitive, as it could detect and explain not only varying damage mechanism differences, but also their strength-diminishing effects.

It is further demonstrated on the basis of examples [39, 50] that defective and defectfree samples differ in a characteristic way in their SE characteristics also in time lapse tests. Both the time interval as well as the intensity of SE registered prior to failure were higher in the case of defective composite materials.

#### Damage Assessment in Cyclic Stress Exposure

In comparison to studies dealing with monotonously increasing stress, there are only few studies examining the suitability of SE measurements for dynamic stress exposure. This is partly due to metrological difficulties encountered in this type of stress exposure (interference noise attenuation, transformer coupling).

Using glass-fiber reinforced NOL-rings, Liptai [29] shows that SE pulse sum increases with increasing load frequency, which indicates continuously progressing damage mechanisms. This finding is confirmed also by Williams and Reifsnider [53] who studied boron fibers/epoxy resin composites. Though they do not deal with SE on the basis of modelling of formation and propagation of defects, they show that there is a proportional relationship between SE pulse sum and the change in dynamic compliance [31-33].

Becht et al. [39, 40] observed in indented three-point bending samples made of GFK (UP-resin/roving tissue) in stress-controlled bending limit tests a relatively strong damage to samples occurring in the first stree cycle (fig. 24) substantiated by SE measurements. An analysis of the signals according to intensity and amplitude /108 distribution identified these damages as delaminations. With continuing load cycles the glass fibers were subjected in the proximity of indentations to an ever increasing stress till they finally broke. Following fiber fracture the SE activity diminished till additional fiber fractures were precipitated by the cummulative effect of the interaction of continuing delaminations. This process repeated itself till final failure of the material. SE was registered only in momentary maximum loads. The authors point out that SE pulse sum is a simply determined value for assessment of potential damage to samples of GFK-laminates exposed to vibration stress. Independent of the position of indentations to fiber orientation (different type of damage) and break-load cycles the pulse sum during an impending break amounts to approximately  $10^6$  counts.

Comparable findings were arrived at also by Roeder et al. [37, 38] who conducted experiments with multilayer systems exposed to dynamic stress. Already after the first load cycle they recorded a higher SE pulse sum than they observed in tests of short duration. They showed by means of an amplitude analysis that damage mechanisms with a higher energy release rate progress in samples exposed to dynamic stress.

## Kaiser Effect

The so-called Kaiser effect is based in irreversibility of SE. As Kaiser proved in his experiments [54], mechanical tension waves are emitted in exposure of a material to repeated stresses only after the initial stress level has been exceeded.

While the existence of the Kaiser effect for a large number of metallic materials is undisputed, some authors question its validity for polymer composite systems [55-57]. Stone and Dingwall [58] carried out experiments using identical conditions and materials as described in [55, 56] and found confirmation for the Kaiser effect. The divergent findings reported in [55, 56] were ascribed by them to inadequacies in the conduct of the experiment.

Rotem and Baruch [28] also confirm with their experiments the existence of the Kaiser effect. Nevertheless, they do point out that the effect is not "clearly" observed at high stress ranges. They ascribe this to the viscoelastic properties of the matrix.

The Kaiser effect is shown in fig. 25 [50]. Following an initially monotonous load increase up to a maximum, the SE activity is spontaneously reduced by load drop (contrary to the experiment shown in fig. 23, in which the load is kept at a maximum). In the subsequent phase of constant load no further emissions are recorded. Only a renewed load increase, which finally leads to failure, strongly activates SE. As can be seen from the arrow in fig. 25, the emissions set in only shortly prior to reaching the level of initial stress exposure.

Liptai [29] as well as Becht et al. [39] observed the Kaiser effect on GFK-wound containers which they exposed to repeated interior pressure cycles.

Williams and Lee [46] point out on the basis of their experiments with carbon fiber/epoxy resin composites that while there was no clear indication of a Kaiser effect due to varying damage mechanisms and their complex interaction, SE activity did gradually decrease with repeated loading and relaxation cycles. They termed this observation as "acoustic emission shakedown."

In evaluation of Kaiser effect experiments consideration must also be given to the fact that SE can also occur as the result of friction processes in damaged fiber/matrix. These emissions can be observed under certain circumstances during loading as well as relaxation processes, but are not in contradiction with explanation of the Kaiser effect.

### Summary

SE monitoring is suited for indication of energy conversion processes in polymer composite materials caused, e.g., by crack formation and crack propagation, under real-time conditions. While pulse sums and pulse rates of SE offer the possibility to monitor the entire progress of damage processes, it is possible to differentiate between the various failure mechanisms by means of corresponding signal analysis of SE. The monitoring process is suited for indication of potential defects in component parts as well as defective materials in testing or inspection of component parts.

Summing up the studies contained in technical literature, there is a wealth of experimental findings and observations which, however, aside from a few exceptions, are seldom quantitatively followed up. SE characteristics are often only tokenly compared with mechanical properties; correlations are not checked. More studies will be required in this area in the future.

It must be further stated that the data regarding experimental parameters of SE monitoring are in part incomplete, so that further interpretation or reproduction of the experiments is not possible. If these studies are to contribute to a common fund of knowledge, such data must be viewed as having a wider significance. Only when there is complete availability of such data can SE experiments be correctly assessed. The checklist proposed by Williams and Lee [46] (table 3) is well suited for documentation of SE experimental conditions and experimental parameters.

Author's address: Reinhard Bardenheier, Deutsches Kunststoff-Institut (DKI), Schlossgartenstrasse 6 R, 6100 Darmstadt

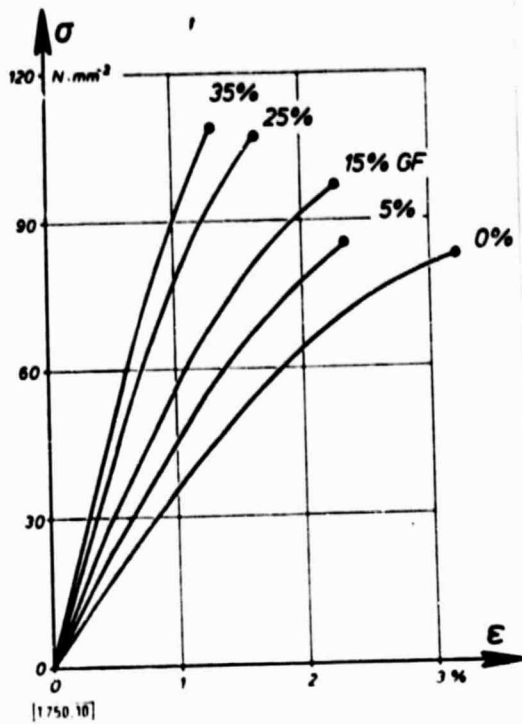


Fig. 10. Mechanical behaviour of a styrene-acrylonitril-copolymer under tensile stresses. Variation in the fibre fraction. Testing speed: 2.5 mm/min (24).

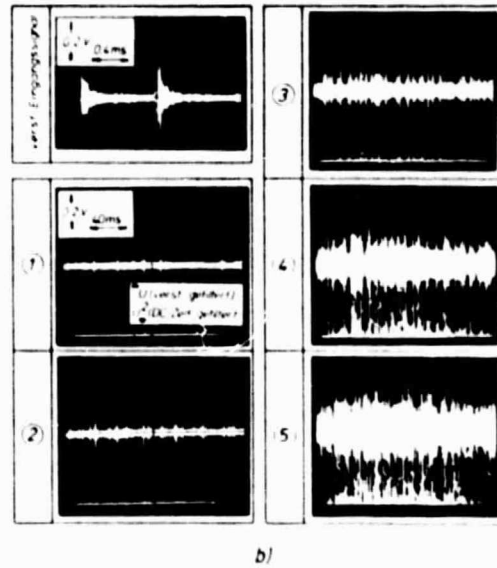
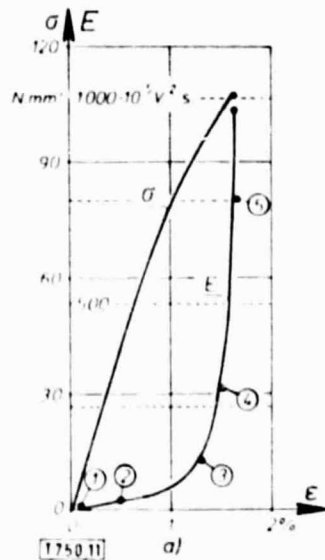


Fig. 11. a) Total energy (E) - and stress ( $\sigma$ ) - strain ( $\epsilon$ ) - diagram of a GF/SAN (25% GF weight fraction). b) Oscillograms. Test conditions: Tensile test, room temperature, testing speed 2.5 mm/min; total signal amplification 55 dB, signal filter 100 kHz Highpass, threshold trigger 200 mV (24).

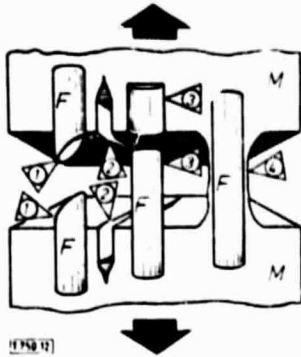


Fig. 12. Failure mechanisms of reinforced polymers: ① Fibre fracture, ② Matrix crazing/matrix fracture, ③ Fibre-pull-out with/without friction, ④ Fibre pull-out and matrix yielding, F: Fibere, M: Matrix.

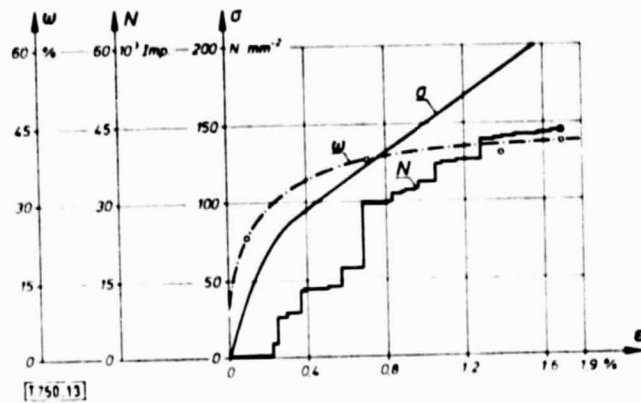


Fig. 13. Summation acoustic emission, percentage of cracked fibres, and stress as a function of strain for a rising load tension test on Al/Ni-whisker reinforced aluminum composite (27). Signal amplification 95 dB, signal filter 100-150 kHz Bandpass.

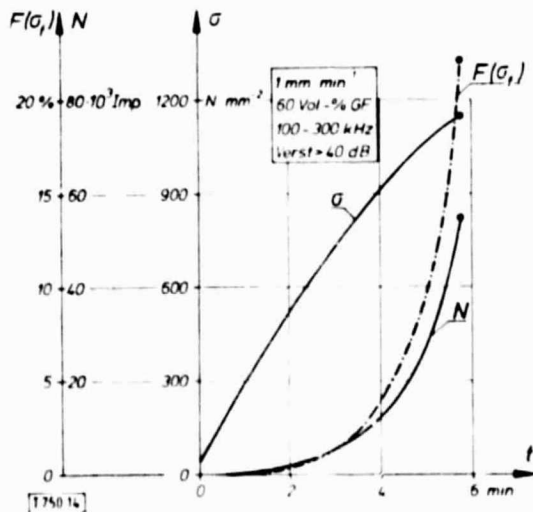


Fig. 14. Acoustic emission monitoring of a tensile loaded, unidirectionally reinforced glass fibre/epoxy composite. Calculated, relative number of fibre fractures  $F(G_f)$  (28).

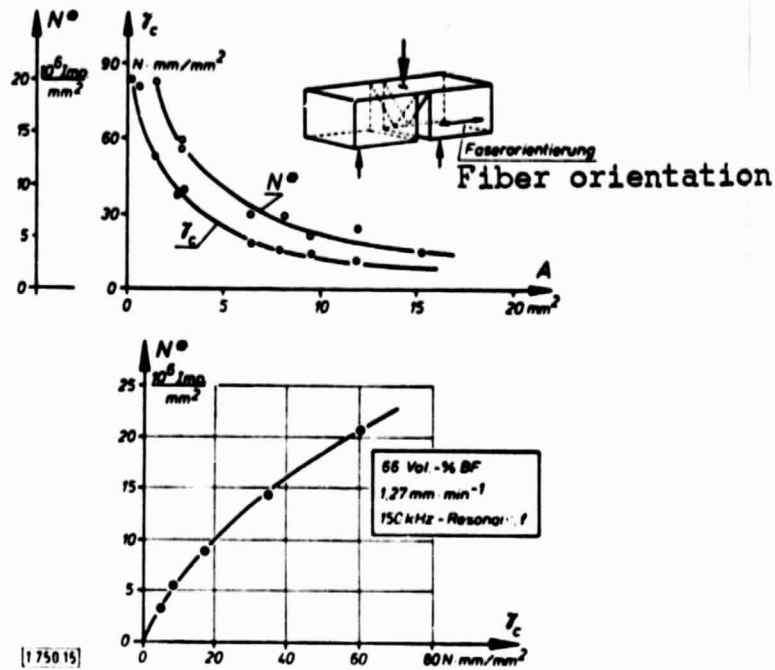


Fig. 15. Fracture energy and acoustic emission of a boron-epoxy-composite (31, 32).

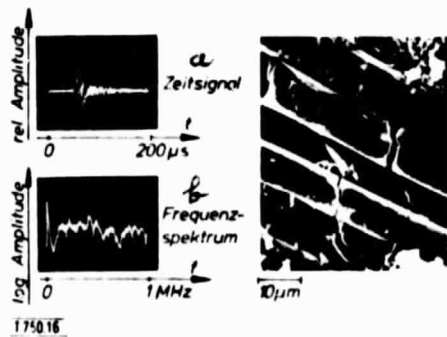


Fig. 16. Fibre fractures and its acoustic emission characteristics, SEM micrograph (36).

Key: a - time signal  
b - frequency spectrum

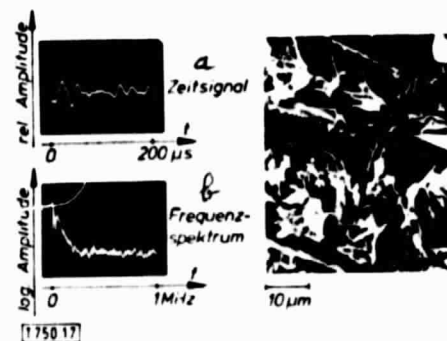


Fig. 17. Delamination processes and its acoustic emission characteristics, SEM micrograph (36).

Key: a - time signal  
b - frequency spectrum



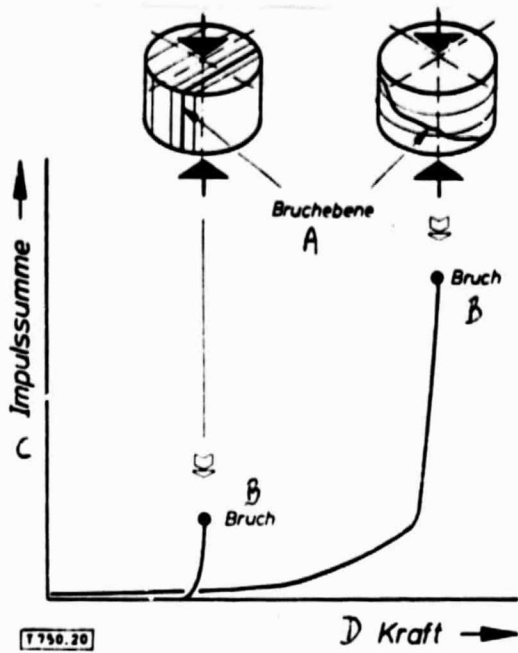


Fig. 20. Acoustic emission of axially compressed glass fibre/epoxy-composites. Fibre sheets parallel and perpendicular to the loading axis (29).

Key: A - plane of fracture  
 B - fracture  
 C - sum of pulses  
 D - force

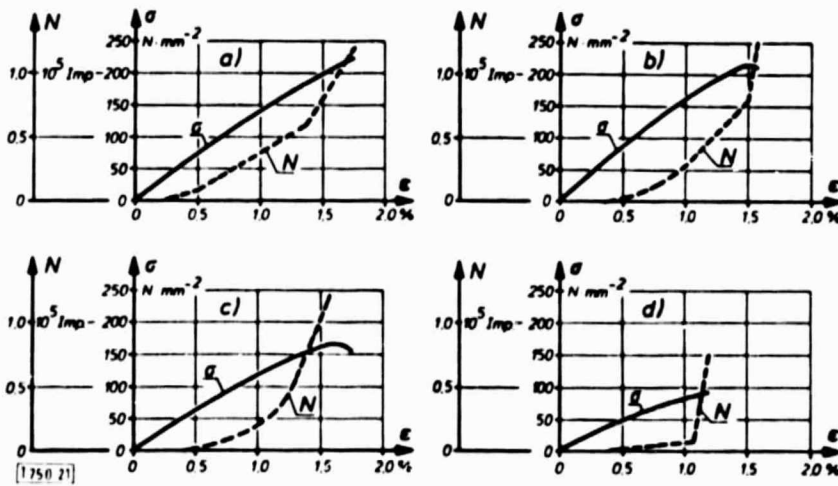


Fig. 21. Stress ( $\sigma$ ) and acoustic emission (number of total counts  $N$ ) as a function of strain ( $\epsilon$ ) for different multilayer-composites (37, 38). Frequency 120-900 kHz, threshold trigger 300  $\mu$ V,  $\epsilon = 1,2\% \text{ mm}^{-1}$ . a) Reinforcement 1:1, b) Reinforcement 1:2 ( $2 \uparrow$ : parallel to the loading axis), c) Reinforcement 2:1 ( $1 \uparrow$ : parallel to the loading axis), d) Reinforcement by mats.

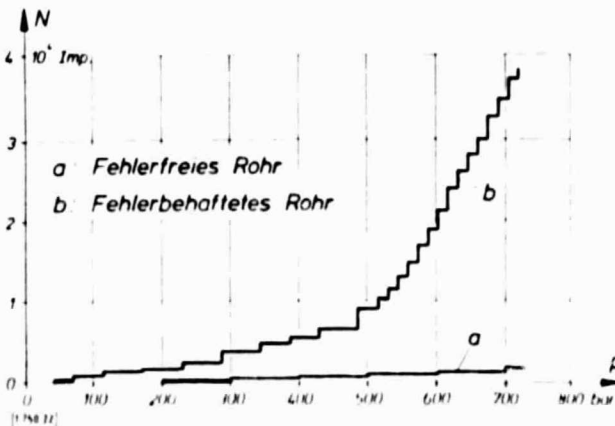


Fig. 22. Total acoustic emission counts of a faulty and fault-free tube at internal pressure (39).

Key: a - defect-free tube  
 b - defective tube

A		B			
Faser	Durchmesser $\mu\text{m}$	$\sigma_{01}$ $10^3 \cdot \text{N/mm}^2$	$\Sigma \sigma_0$ $2 \cdot 10^3 \cdot \text{N/mm}^2$	$\rho$ $2 \cdot \text{g} \cdot \text{mm}^{-3}$	
C	E-Glas	etwa 10	1,5	0,73	2,58
E	S-Glas	etwa 10	3,0	0,81	2,48
F	HM-Glas	etwa 10	3,5	bis 1,17	2,89
G	Asbestos	1 - 100	0,7 - 2,3	1,4 - 1,8	2,5 - 3,4
H	Bor auf Wolfram	100	2,8 - 3,5	4,0	2,65
I	Bor-Silicium-Karbid auf Wolfram	> 100	3,0 - 3,5	4,0	2,7
J	SiC auf Wolfram	100	2,5	4,2 - 4,7	3,35
K	C - HT	7 - 9	2,5 - 3,2	2,2 - 3,0	1,8
L	C - HM	7 - 9	1,5 - 2,3	3,5 - 4,0	1,95
M	Aramidfaser (Kevlar 49)	12	3,0	1,35	1,45
N	Stahldraht	$\geq 50$	3,6	2,1	7,8

Table 2. Properties of fibres

Key: A - fiber, B - diameter,  
 C - E-glass, D - approx.  
 E - S-glass, F - HM-glass  
 G - boron on tungsten  
 H - boron-silicon-carbide  
 I - SiC on tungsten  
 J - aramide fibers  
 K - steel wire

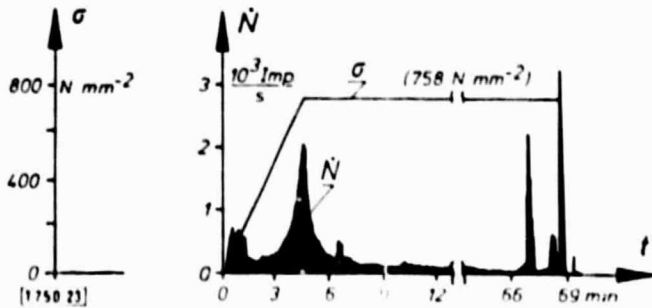


Fig. 23. Count rate ( $\dot{N}$ ) of acoustic emissions of an unidirectionally reinforced glass fibre/epoxy composite at static tensile load ( $\sigma_0$ ).

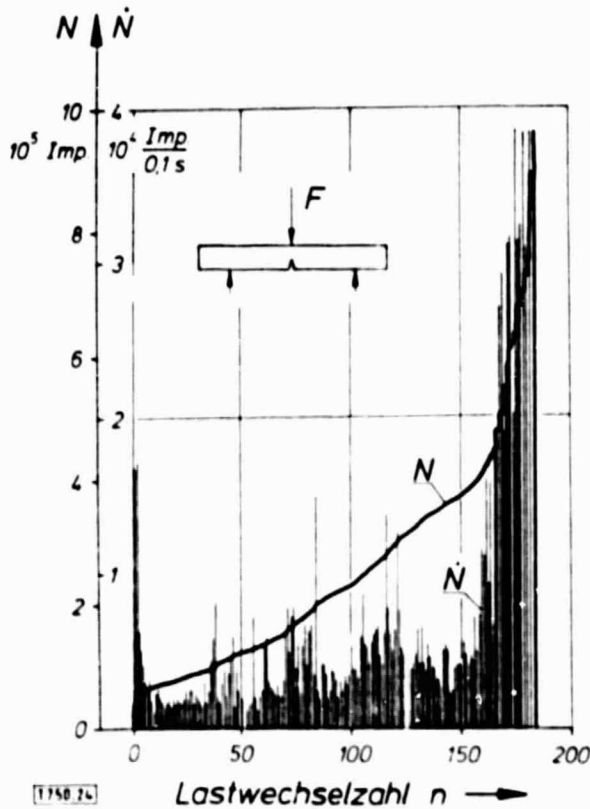


Fig. 24. Count rate ( $\dot{N}$ ) and total counts ( $N$ ) of acoustic emissions at low cycle fatigue loading (39, 40).

number of load cycles

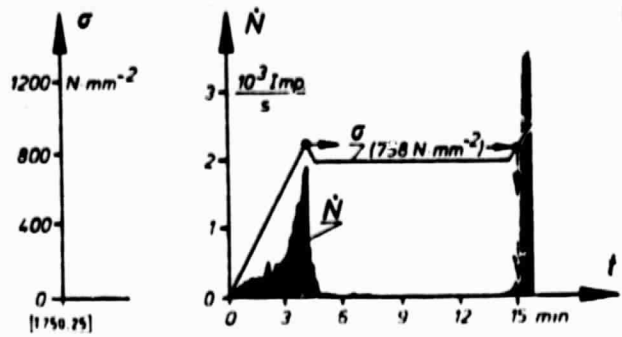


Fig. 25. Kaiser-effect (see arrow) (50).

## REFERENCES

24. Bardenheier, R., "Untersuchungen der Schaedigungsmechanismen glasfaserverstaerkter Styrol-Acrylnitril-Copolymerer mit Hilfe der Schallemissionsanalyse" [Studies of failure mechanisms of styrol-acrylnitrile copolymers reinforced by glass fibers by means of acoustic emission analysis], Kunststoffe 69, 329-333 (1979).
25. Swindlehurst W. E. and C. Engel, "A model for acoustic emission generation in composite materials," Fib. Sci. Techn., 11, 463-479 (1978).
26. Barker, L. M., "A model for stress wave propagation in composite materials," J. Comp. Mat., 5, 140-162 (1971).
27. Harris, D. O., A. S. Tetelman and F. A. I. Darwish, "Detection of fiber cracking by acoustic emission," Techn. Report DRC-71-1, Dunegan Research Corporation.
28. Rotem, A. and J. Baruch, "Determining the load-time history of fibre composite materials by acoustic emission," J. Mat. Sci., 9, 1789-1798 (1974).
29. Liptai, R. G., "Acoustic emission from composite materials," Composite Materials Testing and Design (2nd Conf.), ASTM-STP 497, 285 (1972).
30. Zweben, C. and B. W. Rosen, "A statistical theory of material strength with application of composite materials," J. Mech. Phys. Solids, 18, 189 (1970).
31. Fitz-Randolph, J., D. C. Phillips and P. W. R. Beaumont and A. S. Tetelman, "The fracture energy and acoustic emission of a boron-epoxy-composite," J. Mat. Sci., 7, 289-294 (1972).
32. Fitz-Randolph, J., D. C. Phillips, P. W. R. Beaumont and A. S. Tetelman, "Acoustic emission studies of a boron-epoxy-composite," J. Comp. Mat., 5, 542-548 (1971).
33. Davidge, R. W. and G. Tappin, "The effective surface energy of brittle materials," J. Mat. Sci., 3, 165-173 (1968).
34. Harris, B. and A. O. Ankara, "Cracking in composites of glass fibres and resin," Proc. R. Soc. London A, 359, 229-259 (1978).
35. Mehan, R. L. and J. V. Mullin, "Analysis of composite failure mechanisms using acoustic emissions," J. Comp. Mat., 5, 266-269 (1971).
36. Wolitz, K., W. Brockmann and T. Fischer, "Zerstoerungsfreie Pruefung von Verbundwerkstoffen," [Nondestructive testing of composite materials], Ber. zum 93. Wehrtechn. Symp. "Verbundwerkstoffe in der Wehrtechnik," [Report for 93rd Defense

Technology Symposium on "Composite Materials in Defense Technology," [Mannheim, Bundesakad. Wehrverw. Wehrt. 93.16.01 (1979)].

37. Roeder, E., H. A. Crostack and W. Brockmann, "Langzeitverhalten von GFK (GFUP) bei zyklischer Beanspruchung (Teil 2)," [Long-term behavior of UP-resin/roving tissue under exposure to cyclic stress (Part 2)], Kunststoffberater, 20, 316-318 (1975).
38. Steffens, H. D., H. A. Crostack and E. Roeder, "Schadigungsvorgaenge in mehrschichtigen GFK (GFUP) bei ruhender und zyklischer Belastung und deren Deutung mit Hilfe der Schallemissionsanalyse, in: Verstaerkte Kunststoffe im Maschinen- und Flugzeugbau," [Failure processes in multilayer UP-resin/roving tissue under static and cyclic stress and their detection by means of acoustic emission analysis, in: Reinforced plastics in machinery and aircraft construction], 497-509, Ung. techn.-wissensch. Zentralbibl. u. Dokumentationszentrum (1975).
39. Becht, J., H. J. Schwalbe and J. Eisenblaetter, "Acoustic emission as an aid for investigating the deformation and fracture of composite materials," Composites, 7, 245-248 (1976).
40. Ahlborn, H., J. Becht and H. J. Schwalbe, "Untersuchungen zur 'Risszaehigkeit' verschiedener GFK-Lamine unter Einsatz der Schallemissionsanalyse," [Study of crack-resistance of various UP-resin/roving tissue laminates with the use of acoustic emission analysis], Kunststoffberater, 20, 312-315 (1976).
41. Jax, P., "Schallemission bei plastischer Verformung von Metallen, in: Schallemission -- Berichte zum Symposium der Dt. Gesellschaft fuer Metallkunde," [Acoustic emission in plastic deformation of metals, in: Acoustic emission -- Reports for the Symposium of the German Society for Metallography], DGM-Selbstverlag, 59-117 (1974).
42. Roeder, E. and H. A. Crostack, "Rissbildung in <sup>la</sup>glas- und kohlenstoffaserverstaerkten UP- und EP-Harzen," [Crack formation in UP- and EP-resins reinforced by glass and carbon fibers], Der Maschinenschaden, 50, 121-129 (1977).
43. Weuhreter, A. F. and C. R. Horak, "Acoustic emission system for estimation of ultimate failure strength and detection of fatigue cracks in composite materials," 33rd Ann. Techn. Conf., Washington, Reinforced Plast./Comp. Inst., Soc. Plast. Inst., Sec. 24-B/1 (1978).
44. Fuwa, M., A. R. Bunsell and B. Harris, "An evaluation of acoustic emission techniques to carbon-fibre composites," J. Phys. D: Appl. Phys., 9, 353-364 (1976).
45. Speake, J. H. and G. J. Curtis, "Characterization of the fracture processes in CFRP using spectral analysis of the acoustic emission arising from the application of stress," Int. Conf. on Carbon Fibres -- Their Place in Modern Technology, London, The Plastics Institute, Paper No. 2 (February 1974).

46. Williams, J. H. and S. S. Lee, "Acoustic emission monitoring of fiber composite materials and structures," J. Comp. Mat., 12, 348-370 (1978).
47. Hamstad, M. A. and T. T. Chiao, "Acoustic emission produced during burst tests of filament-wound bottles," J. Comp. Mat., 7, 320-332 (1973).
48. Schwalbe, H. J., "Acoustic emission as an aid for inspecting GFRP pressure tubes," Proc. of 1978 Int. Conf. Comp. Mat., Toronto, 1093-1104 (1978).
49. Rotem, A., Effect of strain rate on acoustic emission from fibre composites," Composites, 9, 33-36 (1978).
50. Hahn, H. T. and R. Y. Kim, "Proof testing of composite materials," J. Comp. Mat., 9, 297-311 (1975).
51. Goettlicher, M., "Untersuchungen zum Schaedigungsverhalten kurzglasfaserverstaerkter Styrol-Acrylnitril-Copolymerer," [Studies of failure behavior of styrol-acrylnitril copolymers reinforced with short glass fibers], Dissertation, Barmstadt, DKI (1979).
52. Crostack, H. A. and E. Roeder, "Ermittlung alterungsbedingten Festigkeitsaenderungen in GFK mittels Schallemissionsanalyse," [Determination of strength changes in composite materials due to ageing by means of acoustic emission analysis], Gummi Asbest Kunstst., 30, 689-694 (1977).
53. Williams, R. S. and K. L. Reifsnider, "Investigation of acoustic emission during fatigue loading of composite specimens," J. Comp. Mat., 8, 340-355 (1974).
54. Kaiser, J., "Untersuchungen ueber das Auftreten von Geraeuschen beim Zugversuch," [Studies regarding Occurrence of Acoustic Emissions in Tensile Tests], Dissertation at the Technical College Munich (1950).
55. Kim, H. C., A. P. Ripper-Neto and R. W. B. Stephens, "Some observations on acoustic emission during continuous tensile cycling of a carbon fiber epoxy composite," Nat. Phys. Sci., 237, 78-80 (1972).
56. Kim, H. C., A. P. Ripper-Neto and R. W. B. Stephens, "Gegengarstellung zum Beitrag (58)," [Rejoinder to Contribution (58)], Nat. Phys. Sci., 241, 69 (1973).
57. Pipes, R. B., N. H. Ballintyn and W. R. Scott, "Acoustic emission response of metal matrix composites," Naval Air Development Center Report, No. NADC - 76022 - 30 (1976).
58. Stone, D. E. W. and P. F. Dingwall, "The Kaiser effect in stress wave emission testing of carbon fiber composites," Nat. Phys. Sci., 241, 68 (1973).